Diamond & Related Materials 113 (2021) 108280

Contents lists available at ScienceDirect

Diamond & Related Materials

journal homepage: www.elsevier.com/locate/diamond

Shift of CO_2-I absorption bands in diamond: A pressure or compositional effect? A FTIR mapping study

Evgenii P. Barannik [a], Andrey A. Shiryaev [b,*], Thomas Hainschwang [c]

[a] Moscow Gemological Laboratory, Arbat St., 30/2, bld. 2, Moscow, Russia
[b] A.N. Frumkin Institute of Physical Chemistry and Electrochemistry, Russian Academy of Sciences, Leninsky pr. 31 korp. 4, 119071 Moscow, Russia
[c] GGTL - GEMLAB Laboratory, Gnetsch, 42, LI – 9496 Balzers, Liechtenstein

ARTICLE INFO

Keywords:
Diamond
CO_2 ice
Infra-red microscopy
Barometry
Impurity

ABSTRACT

Infra-red maps and profiles with high spatial resolution were obtained for two single crystal diamonds with pronounced CO_2 IR absorption peaks. Detailed examination allows unambiguous assignment of the spectral features to solid CO_2-I phase. It is shown that the distribution of IR band positions, intensities and widths in the sample follows regular patterns and is not chaotic as was suggested in previous works where spectra of a few individual spots were analysed. Consequently, pressure effects alone fail to explain all observed features and shifts of the CO_2 bands. Experimental data can be explained by presence of impurities (such as water, N_2, etc.) in the trapped CO_2. This implies that spectroscopic barometry of CO_2 microinclusions in diamond may be subject to poorly controlled bias. However, barometry is still possible if Davydov splitting of the CO_2-I ν_2 band is unequivocally observed, as this indicates high purity of the CO_2 ice.

1. Introduction

Carbon dioxide is an important metasomatic agent in Earth's mantle and plays a major role in the carbon cycle. The presence of CO_2 in diamonds was inferred long time ago from mass-spectrometry studies [1–4]. Presence of carbon dioxide in some gem quality single crystal diamonds follows from IR spectroscopy [5,6] and cryomicroscopy of fluid inclusions [7–9]. Based on the pressure-induced shift of CO_2 peak positions Schrauder and Navon [6] inferred extremely high residual pressures reaching 5 GPa in one specimen, suggesting the presence of compressed solid CO_2. Even higher residual pressures, up to 20 GPa, were mentioned in an extensive investigation of CO_2-containing diamonds by Chinn [5]. In that work strong variations in the shape of the CO_2-related bands between different samples and even between analysis points in the same specimen were reported.

Investigation of a large set of polished diamonds with CO_2 IR bands (termed as "CO_2 diamonds") using a beam condenser, i.e. allowing analysis of relatively small spots, revealed high variability of positions, widths, and relative intensities of CO_2 ν_3 and ν_2 bands [10,11]. These authors suggested that such a variability cannot be explained by the presence of CO_2 phase inclusions and tentatively proposed integration of CO_2-molecules in the diamond lattice. The presence of oxygen as a lattice impurity in diamond is plausible ([12] and references therein, [13]), but its correlation with the CO_2-absorption is uncertain. In this work, we report the results of a detailed investigation of diamond single crystals possessing CO_2 absorption bands using IR microscopy and discuss implications for diamond studies and for more general application of barometry of fluid inclusions in minerals based on spectroscopic data.

2. Samples and methods

Two CO_2-rich diamonds — FN7112 and FN7114 — were studied. Diamond FN7114 was described in Hainschwang et al. [11]. The samples were obtained commercially and their source is unknown. The stones were laser cut from gems and subsequently polished to make a double-sided plate. Both samples were treated at 6 GPa and 2100 °C for 10 min; the treatment did not influence the color and CO_2-related absorption [11]. The sample FN7112 is 3.16 mm in diameter and 0.89 mm thick (mass 0.08 ct); the FN7114 dimensions are 2.51 mm and 1.03 mm (mass 0.06 ct), respectively. According to our previous X-ray topography study [12], the samples are single crystals.

FTIR spectra were collected with a Nicolet iN10 FTIR microscope equipped with a liquid N_2-cooled MCT detector. The microscope and

* Corresponding author.
E-mail address: shiryaev@phyche.ac.ru (A.A. Shiryaev).

https://doi.org/10.1016/j.diamond.2021.108280
Received 21 September 2020; Received in revised form 9 January 2021; Accepted 11 January 2021
Available online 30 January 2021

sample compartment were continuously purged with dry high-purity N_2 before and during spectral acquisition. Although strongly suppressed, traces of CO_2 gas were still observed in spectra. Assuming that this gas signal was from atmospheric contamination, a component of CO_2 gas (represented by the ν_2 and ν_3 bands) was included in the fit. The absorption of gaseous CO_2 for each spectrum was chosen in a way to minimize the difference between the experimental data and the model. This procedure is possible, firstly, because the shape of gaseous CO_2 absorption is known from independent atmospheric measurements, and secondly, because the bands of gaseous CO_2 and CO_2-I overlap only partially. All measurements were performed in transmission mode on free-standing samples at room temperature. For consistency, the microscope was focused on the upper surface of the sample. For the mapping, a square 150 × 150 μm^2 aperture and 100 μm step were used. For the profiles a 30 × 30 μm^2 aperture and 30 μm step were used. Due to high refractive index of diamond, the thickness-averaged size of the analyzing IR beam somewhat deviates from the quoted aperture size. Spectra were acquired in the 600–4000 cm^{-1} spectral range. At least 64 scans per spectrum at a resolution of 2 cm^{-1} were recorded.

FTIR spectra were processed using a custom Lua script for Fityk software [14]. The absorbance measurements were normalized to lattice absorption of a reference type IIa diamond sample; after the normalization, the spectrum of the type IIa reference was subtracted. Linear baseline correction was performed for each zone of interest. Most CO_2-related bands (ν_{2a}, ν_{2b}, $^{13}CO_2$ ν_{3b}, ν_{3a}) as well as carbonate and platelet bands were fitted with Gaussian distributions. Positions of relevant CO_2-related absorption bands are summarised in Table 1. The CO_2-I ν_{3b} band was approximated by two Gaussians with identical position. A Voigt profile was used for the peak at 3107 cm^{-1} (tentatively assigned to a VN_3H-center, [17]). Concentrations of nitrogen in A and B form were calculated after spectral decomposition in the one-phonon region and using coefficients from Boyd et al. [18] and Kiflawi et al. [19]. Tentative identification of minerals in inclusions was made using compilation by Chukanov and Chervonnyi [20]. Plots and maps were created using Matplotlib library for Python [21]. All raw and processed FTIR spectra are available as Supplementary Materials.

3. Results

3.1. The samples

Both studied diamonds are single crystals with a light greenish-brown color. Diamond FN7112 shows faint yellow fluorescence under ultraviolet light excitation, while diamond FN7114 is inert. The diamonds contain tiny inclusions of roughly hexagonal shape with dimensions of 5–10 μm and thickness of less than a micron (Fig. 1). In sample FN7112 the inclusions are present in the whole body of the stone and are crystallographically oriented; in some regions larger plates appear to be surrounded by smaller ones, possibly indicating that decrepitation of some inclusions has occurred. In sample FN7114 the inclusions occur in clusters of up to ~10 plates. It is important to emphasize that there is no obvious correlation between abundance and distribution of these inclusions and infra-red features (including CO_2-related bands) described below. Similar inclusions were reported by Lang et al. [22] and Hainschwang et al. [23] and ascribed to graphite.

Table 1
Assignment of the CO_2-related bands [15,16].

Position (cm^{-1})	Band	Assignment
650	ν_{2b}	CO_2-I, bending (ν_2) mode
660	ν_{2a}	CO_2-I, bending (ν_2) mode
2299–2305	$^{13}CO_2$ ν_{3b}	CO_2-I, $^{13}CO_2$ analog of the ν_3 mode
2369–2375	ν_{3b}	CO_2-I, symmetric stretching (ν_3) mode
2415	ν_{3a}	Uncertain
3615	$\nu_3 + 2\nu_2$	CO_2-I, overtone
3740	$\nu_3 + \nu_1$	CO_2-I, overtone

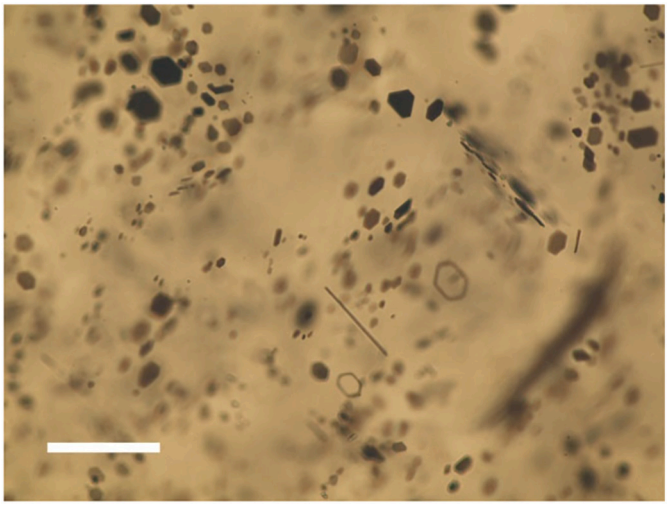

Fig. 1. A photomicrograph of inclusions in diamond FN7112 in transmission light; scale bar – 50 μm. One can see numerous (quasi)hexagonal inclusions and rare needle-like ones (e.g., a ~40 μm-long one slightly below center of the image). Some of the inclusions do not contain dark material and at least in some cases they are very close to the surface of the stone, thus pointing to influence of the polishing on loss of the material (possibly due to heating).

Raman microscopy of the inclusions (excitation 532 and 785 nm), X-ray diffraction, X-ray fluorescence and phase tomography have not provided useful information, thus unambiguous identification of the inclusions is not yet possible. However, the hypothesis of the presence of graphite or other types of sp^2-carbon in the inclusions now appears to be less sound, given the high sensitivity of Raman spectroscopy with visible excitation to sp^2-C and the absence of any relevant features in our spectra. In addition, needle-like inclusions with length up to ~40 μm are also present (see also [23]). The later ones clearly do not correspond to the hexagonal plates viewed edge-on as suggested by careful examination under several inclination angles and generally larger sizes of the needles.

In both samples unusual absorption features between ~900–1400 cm^{-1} (one-phonon region) which cannot be ascribed to known nitrogen-related defects are observed (Fig. 2). Maxima of the bands are at 1060, 1120–1140, ~1245, ~1300 cm^{-1}, and a broad band with a maximum at ~1375 cm^{-1} may also be related to this set of absorptions. A sharp peak at 1332 cm^{-1} (Raman frequency of diamond) is always present, but its unique assignment is barely possible, since in crystals with diamond structure this vibration becomes IR-active in the presence of any defect, violating point symmetry of the matrix [24]. These absorption bands were discussed in a previous study of CO_2-diamonds [11]. Similar features were observed in a recent study of diamonds from Chidliak, Canada [25]; no microinclusions were observed microscopically in these samples (Lai, pers. comm). Broad bands, possibly related to water or OH-containing groups in inclusions, are observed in the 1450–1750 and 3200–3700 cm^{-1} spectral regions for both samples (Fig. 2). Attempts to establish correlations between OH-related and carbonate bands were abandoned due to interference of broad bands with unknown origin, shapes and intensities.

Below we discuss in detail the spectral features of the studied diamonds.

3.2. Diamond FN7112

A photomicrograph of the sample is shown in Fig. 3A. The FTIR spectra of specimen FN7112 show carbonate (870 and 1430 cm^{-1}) and 800 cm^{-1} (possibly a silicate, e.g. quartz) bands, weak peaks at 3107 cm^{-1} and 3272 cm^{-1}; maps of some of these features are shown in Fig. 3B–D. Absorption by nitrogen-related A, B or C-defects is not detected. The bands at 650, 660 and 2370 cm^{-1} are due to CO_2 ν_{2a}, ν_{2b},

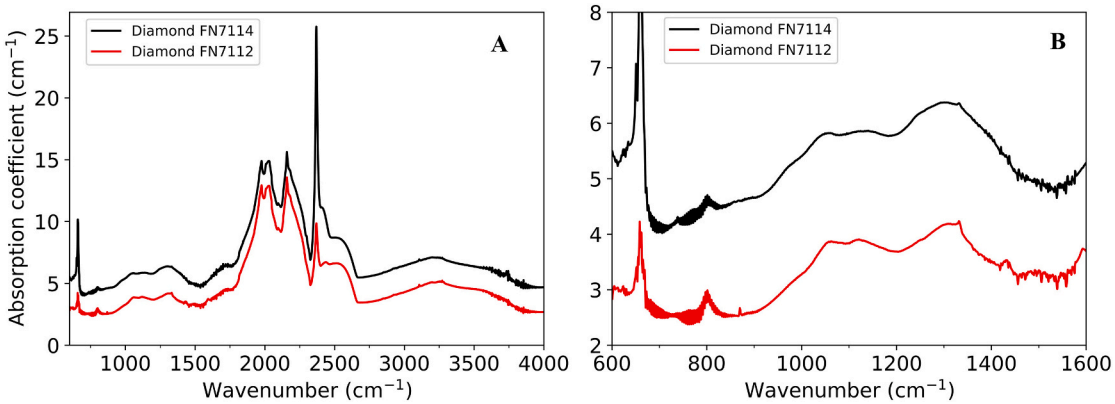

Fig. 2. Typical FTIR spectra of the studied diamonds showing analysis points with CO_2-related absorptions. A – The whole recorded range, B – one-phonon region. For diamond FN7114, the spectrum of the brown zone is shown. For clarity, the spectrum of the specimen FN7114 is vertically displaced by 2 cm^{-1}.

and ν_{3b} vibrations (Fig. 4A, B); weak features at ~3615 and ~3740 cm^{-1} are $\nu_3 + 2\nu_2$ and $\nu_3 + \nu_1$ overtones, respectively (Fig. 4E). A very weak feature at 2300 cm^{-1} is due to $^{13}CO_2$ ν_{3b}. The bands show no rotational splitting and are shifted from the position of gaseous carbon dioxide. We assign these bands to the CO_2-I phase, see Discussion for detail. The most intense of the bands, the ν_{3b}, appears symmetrical. In some spectra a shoulder at 2350 cm^{-1} due to residual CO_2 gas in the spectrometer is visible.

The integrated area of the CO_2-I bands varies significantly across specimen FN7112 as shown by maps of ν_{2b}, ν_{2a} and ν_{3b} peaks (Fig. 3E–G). The CO_2 distribution is unrelated to strain observed in polarized light, but inversely correlates with intensity of the coloration: the CO_2 bands are stronger in less intensely colored zone. Apparently, the number of visible hexagonal inclusions is not correlated with the intensity of CO_2 absorption.

3.3. Diamond FN7114

FN7114 is a diamond with distinct zoning; brown, yellow and (near) colorless zones are distinguished; IR-active features generally follow the zoning (Fig. 5). The colorless zone shows absorption by A, B-defects and platelets, superposed on unassigned bands (see Section 3.1). The three-phonon region possesses a complex shape between 3100 and 3300 cm^{-1} with peaks at 3107, 3272 and very weak features at 3144, 3200, 3238, 3257 cm^{-1}. The ~800 cm^{-1} band is rather uniformly distributed. Carbonates (possibly calcite) are detectable near the black feature visible in the right half of the diamond, which probably represents a healed fracture.

It is convenient to discuss changes of the spectral features in different zones of the specimen using profile across the sample shown by vertical arrow in Fig. 5A; evolution of various features is shown in Figs. 6 and 7. Peaks due to carbon dioxide vary considerably in intensity and shape between the zones (Figs. 5, 6). The colorless zone shows weak CO_2-I bands; the yellow zone exhibits the strongest CO_2-I absorption and the brown zone spectra show a weak CO_2-I band with an additional feature at 2415 cm^{-1} (Fig. 6). Assignment of the band at 2415 cm^{-1} (ν_{3a}) is uncertain, but several possibilities are examined in the Discussion section. In addition, a small band at 2300 cm^{-1} is observed. We assign it to the ν_3 vibration of isotopically-substituted carbon dioxide molecule, i.e. $^{13}CO_2$ ν_{3b}; the supporting evidence is given in the Discussion section.

Along the profile, the CO_2-I ν_{3b} band broadens (FWHM increases from 20 to 55 cm^{-1}) and its center shifts from 2369 to 2375 cm^{-1}; the $^{13}CO_2$ ν_{3b} isotopic band behaves in a similar way (Fig. 6). The position of the ν_{2a} band does not change significantly, while its FWHM increases from 8 to 17 cm^{-1}. Upon broadening of the more intense ν_{2a} band, the ν_{2b} component turns into a shoulder, introducing uncertainty into its position for the zone containing nitrogen defects.

Examination of distribution of the CO_2-related and carbonates bands does not allow establishing a solid correlation. Whereas for diamond FN7112 these phases might be correlated, for sample FN7114 no relation is apparent. Therefore, it is unclear whether CO_2-carbonate correlation exists.

Fig. 7A shows evolution of integrated areas of the CO_2-related bands and nitrogen concentration along the profile. At the transition from the brown to yellow zone (points 20–30), the absorption of CO_2-I rapidly increases and the ν_{3a} band disappears. Simultaneously, defect-related bands in the 900–1400 cm^{-1} region undergo a complex shape change; total absorption diminishes; the peak at 1332 cm^{-1} becomes more prominent. In the same time, absorption in the ranges 1450–1750 and 3200–3700 cm^{-1} becomes stronger.

Since the studied sample represents a laser-cut polished piece of a gem diamond, identification of the growth direction is not trivial. X-ray topography does not reveal obvious growth dislocations, partly due to the moderate degree of plastic deformation. However, examination of a plot of nitrogen concentration vs N aggregation state (Fig. 7B) might give a clue. If one assumes that the diamond growth proceeded in a gradually cooling system, the N aggregation plot suggests that the N-containing zone reflects late stages of the crystal formation. This does not necessarily imply absence of N in the growth medium; it rather indicates unfavorable conditions for incorporation of this impurity. The content of N in the form of common A and B defects gradually increases towards the end of the profile (Fig. 7A). We note, however, that any hypothesis about the N concentration in the FN7114 diamond may be somewhat simplistic, since we do not know yet whether the defects giving rise to absorbance in the one-phonon region contain nitrogen or not.

4. Discussion

4.1. Band assignment

4.1.1. Major CO_2-I bands

At room temperature, CO_2 crystallizes into a cubic phase I between 0.6 GPa and 2 GPa [15,27]; the variations in the transition pressure are ascribed to the size of the CO_2 droplets and, possibly, the nature of the surrounding medium. In the pressure range of ~8–13 GPa a transition into orthorhombic CO_2-III occurs [15]. Fundamental modes and, consequently, IR spectra of these phases differ. The IR spectrum of CO_2-I shows two bending bands (ν_{2a}, ν_{2b}) and a single asymmetric stretching band (ν_3). The CO_2-III spectrum is characterized by splitting of the fundamental modes, showing in total three bending and two stretching bands. With increasing pressure, the stretching and bending vibrations have positive and negative shifts, respectively, in both phases I and III [15,28]. If the ν_2 and ν_3 bands observed in our work indeed arise from

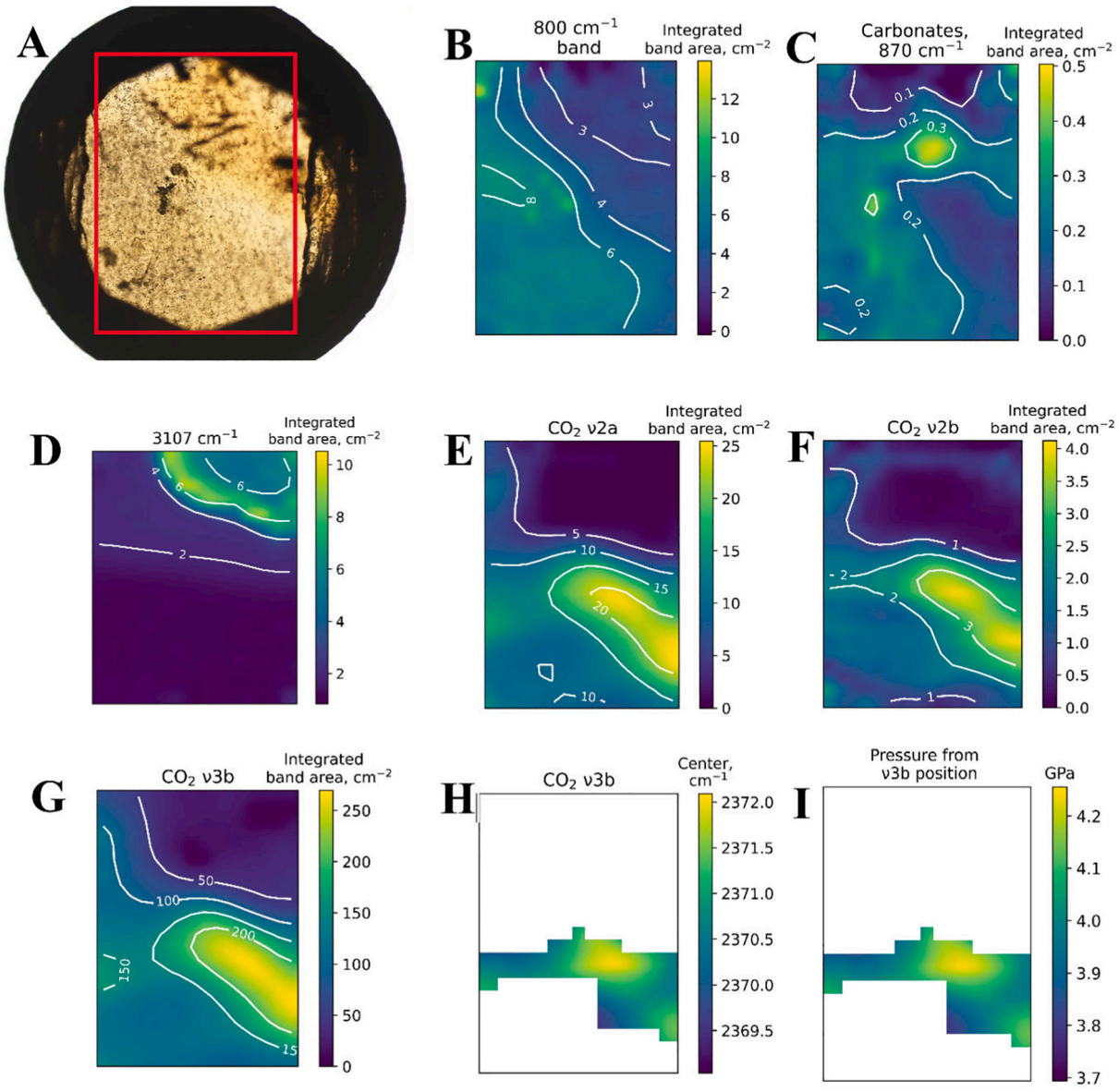

Fig. 3. General view and FTIR maps of diamond FN7112. A – Photomicrograph; red rectangle shows the position of the FTIR maps. Specimen diameter is ~3.1 mm. Black rim is due to extinction in the crown; darkened roughly vertical fields to the right and left of the red rectangle – supporting polymer film. The FTIR maps are shown with a slightly changed aspect ratio and size than area marked on A. FTIR spectra of "black" mapped regions were obtained according to the standard procedure. B – Integrated area of 800 cm^{-1} band, C – integrated area of carbonate band; D – integrated area of 3107 cm^{1} peak. E–G – integrated areas of CO_2-related bands; H – position of ν_{3b} band; I – residual pressure in CO_2 inclusions calculated assuming absence of other factors influencing ν_{3b} band position (see text for detail).

the CO_2–I phase, a linear correlation between their areas is expected. Fig. 8 shows correctness of this assumption for both samples. We emphasize that the spectra of the brown zone in diamond FN7114 show two main components in the ν_3 region — ν_{3a} and ν_{3b}. Only ν_{3b} appears to correspond to the CO_2-I phase; areas of ν_{3a} and CO_2-I bands are inversely correlated. Based on the observed number of bands, positions and (ν_{2b} + ν_{2a}) to ν_{3b} area correlation, we can confidently assign ν_{2b}, ν_{2a}, ν_{3b} to the CO_2-I phase.

A ν_{2b} band centered at 650 cm^{-1} contributes up to 15% to the ν_{2a} (660 cm^{-1}) area. It behaves differently from that of ν_{3b} and the 2415 cm^{-1} peak (the ν_{3a} band, see below), transforming into a shoulder in the nitrogen-rich zone of the diamond. The ν_{2a} and ν_{2b} bands correspond to CO_2 bending influenced by Davydov splitting. Lattice disorder markedly influences the magnitude of the Davydov splitting in molecular crystals. In particular, addition of 10% of H_2O into CO_2 ice leads to suppression of the splitting [29]. Consequently, the presence of distinct ν_{2b} absorption may indicate purity of CO_2-ice in inclusions.

4.1.2. Isotopic $^{13}CO_2$-I ν_{3b} band

A weak band at 2300 cm^{-1} (Fig. 4B,D) is observed in the whole mapped region of sample FN7114 (Fig. 5N) and in zones with relatively high CO_2 absorption in diamond FN7112. The measurement of the 2300 cm^{-1} band is complicated due to its superposition on intrinsic diamond absorption bands. For the profile across the sample FN7114, the area of 2300 cm^{-1} band was measured to be 0.5–1.2% of ν_{3b} area. This band is redshifted 70 cm^{-1} from the CO_2 ν_{3b} peak and its position varies along the profile from 2299 to 2305 cm^{-1} whereas the ν_{3b} peak shifts from 2369 to 2375 cm^{-1}. The FWHM and spatial distribution of the ν_{3b} and 2300 cm^{-1} bands behave in a similar manner. In harmonic approximation, substitution with a heavy isotope should redshift absorption bands and the area of the relevant band should correspond to the isotopic fraction, i.e. ~1.1% in the case of carbon. For crystalline CO_2 the ν_3

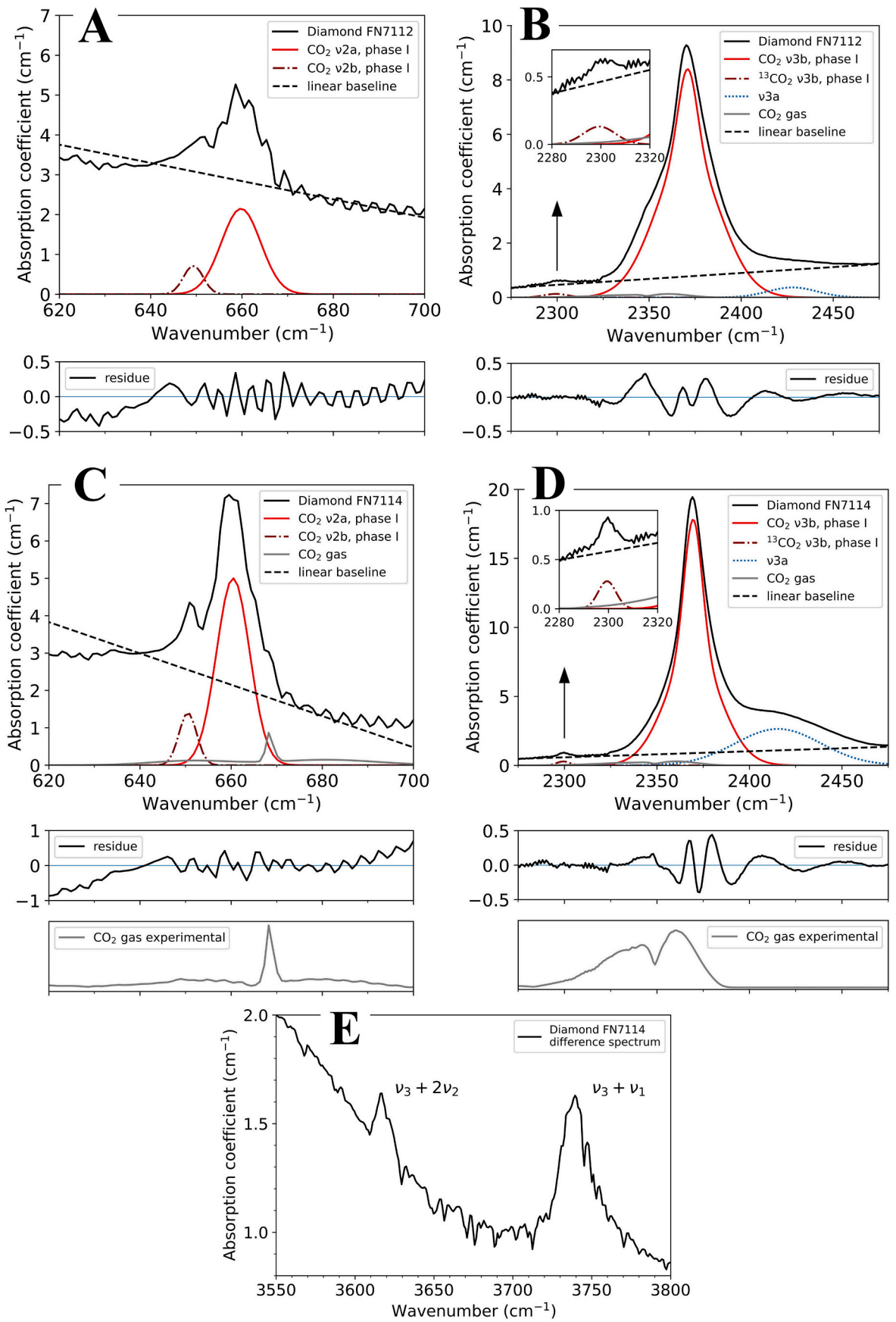

Fig. 4. CO_2-related bands in FTIR spectra of the studied diamonds. A–D – Examples of spectral decomposition for ν_2 and ν_3 regions. A, B – diamond FN7112; C, D – diamond FN7114. Experimental atmospheric spectra are shown for comparison. Residues show the difference between experimental data and the model. E – High frequency part of a diamond FN7114 spectrum.

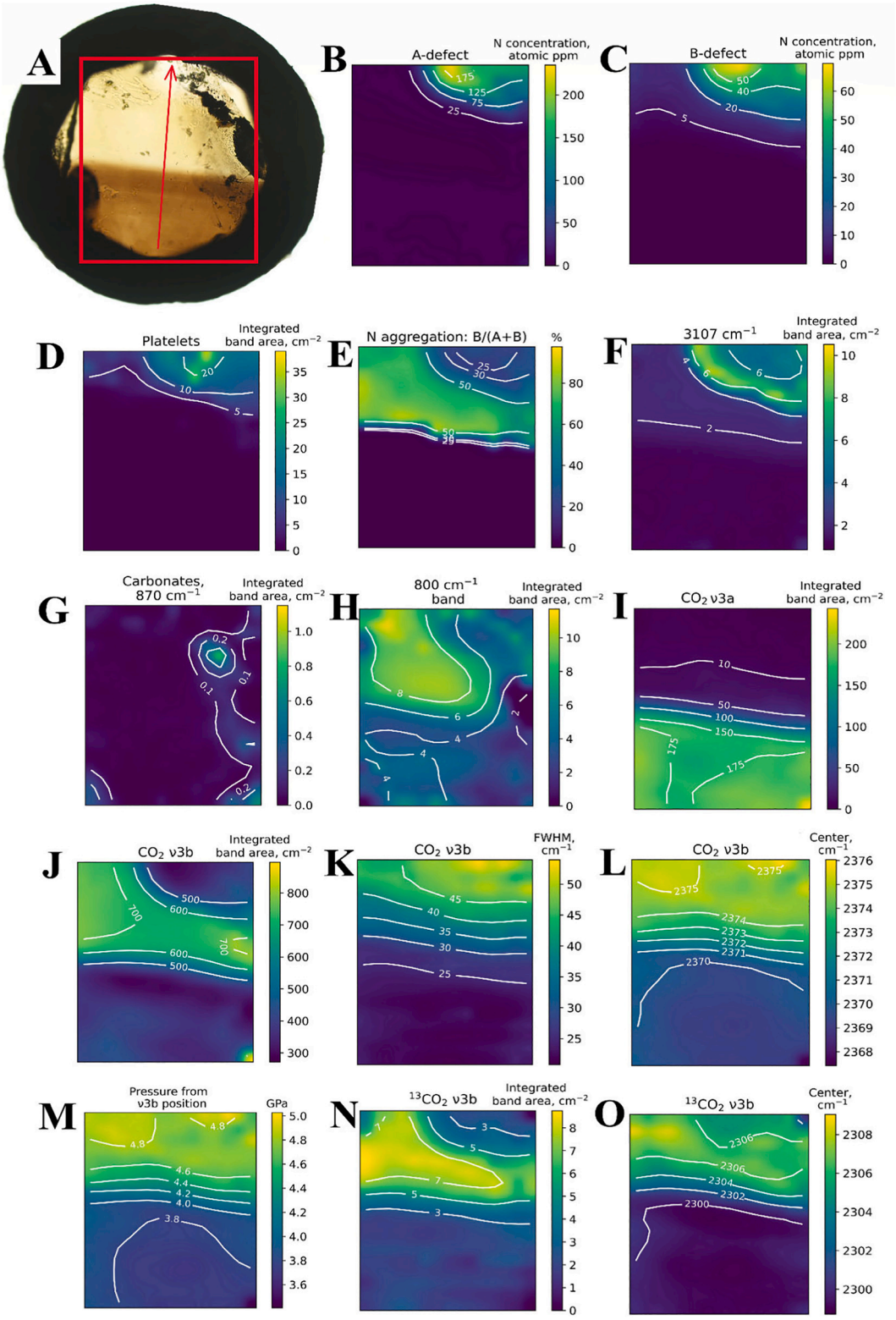

Fig. 5. General view and FTIR maps of diamond FN7114. A – Photomicrograph; red rectangle shows the position of the FTIR maps, arrow indicates direction of the profile. Specimen diameter is ~2.5 mm. Black rim is due to extinction in the crown; darkened roughly vertical fields to the left of the red rectangle – supporting polymer film. The FTIR maps are shown with a slightly changed aspect ratio and size than area marked on A. FTIR spectra of "black" mapped regions were obtained according to the standard procedure. FTIR maps: B, C, D, F – distribution of defects (see notations). E – Nitrogen aggregation. Inclusions: G – integrated area of carbonate band; H – integrated area of 800 cm^{-1} band. I–O – CO_2-related bands. I – Integrated area of ν_{3a} band; J–L – integrated area, FWHM and position of ν_{3b} band. M – Residual pressure in CO_2 inclusions calculated assuming absence of other factors influencing ν_{3b} band position (see text for detail). N, O – Integrated area and position of $^{13}CO_2$ ν_{3b} band.

$^{13}CO_2$ band is located at 2283 cm^{-1} and is redshifted 62 cm^{-1} from ν_3 $^{12}CO_2$ peak at 2345 cm^{-1} [30]. Based on the observed changes in intensity, position and width, the 2300 cm^{-1} band can be assigned to the ν_{3b} mode of $^{13}CO_2$; thus we denote the 2300 cm^{-1} band as $^{13}CO_2$ ν_{3b}.

4.1.3. The 2415 cm^{-1} (ν_{3a}) band

A band at 2415 cm^{-1} denoted as ν_{3a} [5] is observed in spectra of FN7114, but is practically absent in spectra of diamond FN7112 (Fig. 4B, D). This band can be enhanced by HPHT treatment of CO_2 diamonds [11]. According to our data, the ν_{3a} band area can reach 70% of the ν_{3b}. Analyzing its behavior along the profile, one can see that this band is relatively intense in the brown part of the sample FN7114, but almost disappears closer to the N-containing zone. The gradual disappearance of this band correlates with an increase of broad features in 3200– 3700 and 1450–1750 cm^{-1} ranges (possibly, OH-related) and a weak peak at 800 cm^{-1}. Judging from spectra with prominent 2415 cm^{-1} band, its position and FWHM (~55 cm^{-1}) are approximately constant. The assignment of this band is uncertain, but several possibilities are discussed below.

Hainschwang et al. [11] assigned the ν_{3a} band to a highly shifted ν_3. However, detailed examination shows that the ν_{3a} band cannot be assigned to the CO_2-I or CO_2-III macroscopic phases. The value of 2415 cm^{-1} exceeds wavenumbers possible for CO_2-I phase as it would imply pressures outside of the CO_2-I stability field. For the CO_2-III phase an increase of pressure from 9 to 20 GPa shifts ν_3 bands from 2408 to 2436 cm^{-1} and from 2351 to 2369 cm^{-1} [15]. The assignment of the 2415

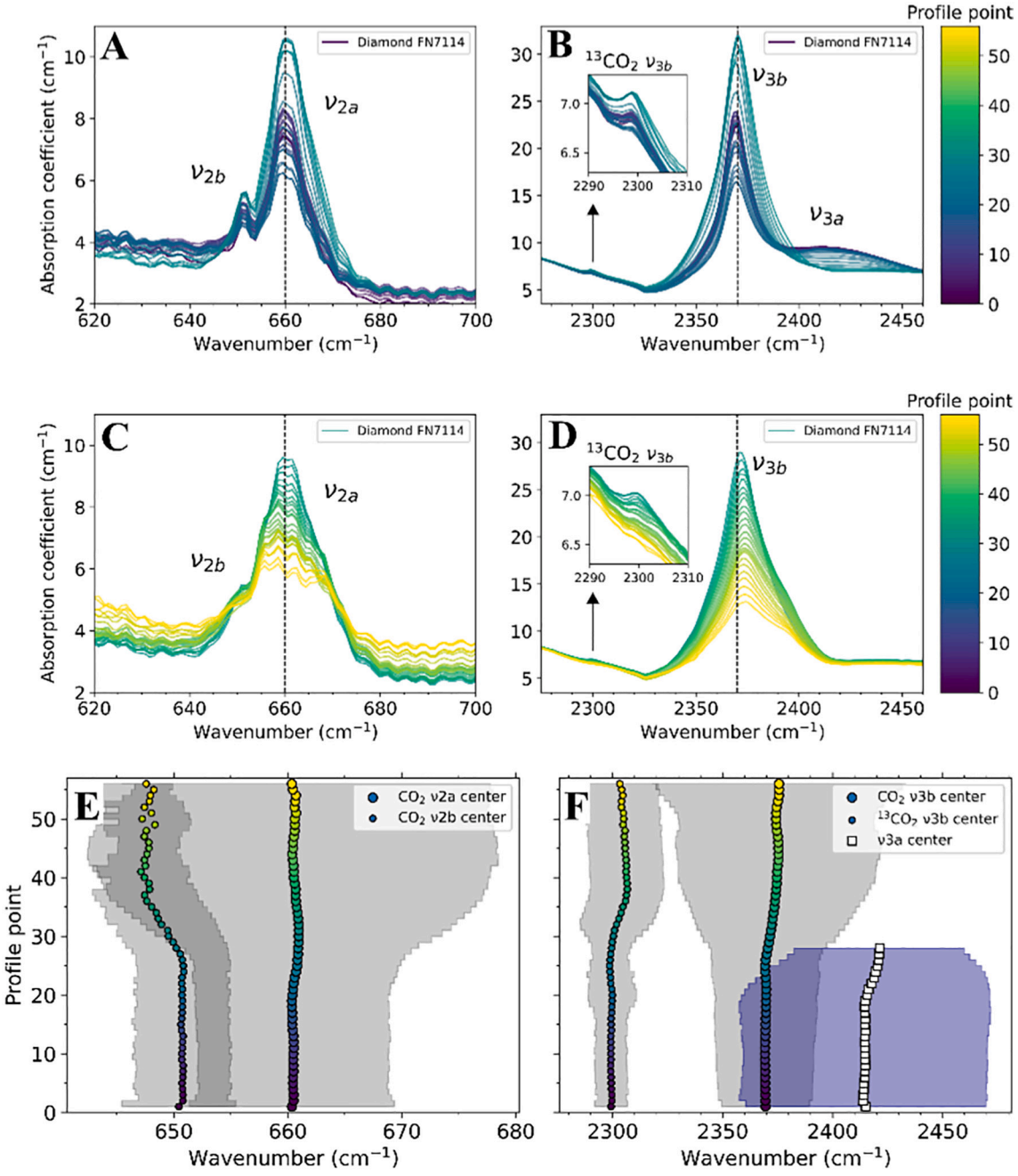

Fig. 6. Evolution of CO_2-related bands in FTIR spectra along the profile across diamond FN7114. For A–D spectra are normalized, but no other manipulations are performed. A, B – Spectra of the brown zone. C, D – Spectra of the yellow and colorless zones. Dashed vertical lines at 660 (A, C) and 2370 cm^{-1} (B, D) are provided for visual reference. E, F – Changes in band position and FWHM. Markers show band center positions; shaded regions are set to ±FWHM. The color scheme shows profile point number.

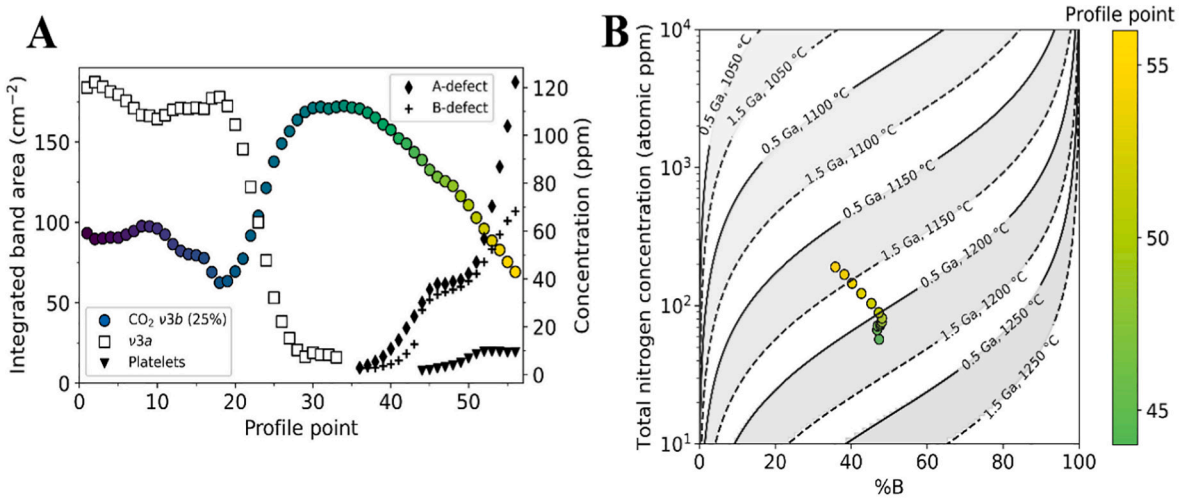

Fig. 7. Evolution of CO_2 and N-related IR features along the profile across diamond FN7114. A – Concentration of nitrogen-related defects, areas of ν_{3a} and CO_2-I ν_{3b} bands (the area of CO_2-I ν_{3b} band is multiplied by 0.25). B - Nitrogen aggregation plot for diamond FN7114. The activation energy and Arrhenius constant are from Taylor et al. [26]. The data are corrected for laboratory-based HPHT annealing described by Hainschwang et al. [11]. The color scheme shows profile point number.

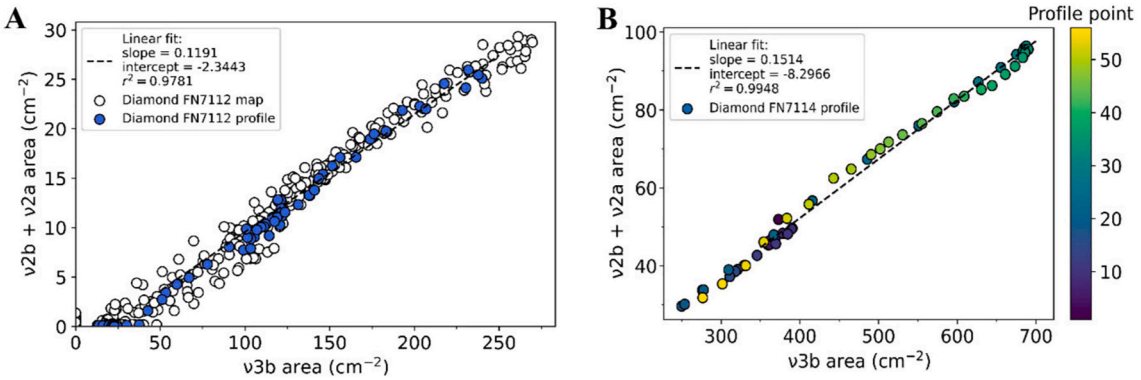

Fig. 8. Correlation of the integrated areas of CO_2 ν_2 and ν_3 bands for studied diamonds. A – $\nu_{2a} + \nu_{2b}$ and ν_{3b} bands for diamond FN7112. Datasets for both map and profile through diamond FN7112 are shown. B – $\nu_{2a} + \nu_{2b}$ and ν_{3b} bands for diamond FN7114.

cm^{-1} band to the CO_2-III phase would also imply existence of a more intense feature centered at ~2355 cm^{-1}, which is actually absent. Secondly, the CO_2 bending mode in spectra from sample FN7114 is doubly split, showing only ν_{2a} and ν_{2b} components, excluding the CO_2-III phase. However, the ν_{3b} and ν_{3a} bands appear to be closely linked. Fig. 7A shows that areas of ν_{3a} and ν_{3b} bands are inversely related by a factor of 2–3. Moreover, if the ν_{3a} band is assigned to a shifted ν_3, the linear dependence between the ν_2 and ν_3 area is violated for sample FN7114 (Fig. 9). If we assume that the ν_{3a} band is not related to the ν_3 mode of CO_2-I, the linearity is restored.

The 2415 cm^{-1} band could be a ν_3 LO (longitudinal optical) phonon mode, provided that the thickness of the substance is sufficiently small and/or the incident IR beam is not perpendicular to the CO_2 film surface [31]. At low temperatures in pure CO_2 ice the LO phonon is blueshifted 39 cm^{-1} from the TO (transverse optical) mode. The shape and maximum position of the LO band depends on the presence of impurities in the ice [32]. It should be noted, however, that we do not observe features unambiguously assigned to the ν_2 LO phonon mode.

And last but not least, the ν_{3a} feature may represent hydrogen bonds in hydrogen carbonates. For example, bands with important features in the relevant spectral range are observed in $CO_2 \cdot H_2O$ complex and carbonic acid [33]; broadly similar spectra are reported for $KHCO_3$ single crystal [34]. Albeit it readily decomposes at ambient conditions, carbonic acid is stable at pressures of several GPa and rather high temperatures [35,36]. Of course, IR spectra of both carbonic acid and

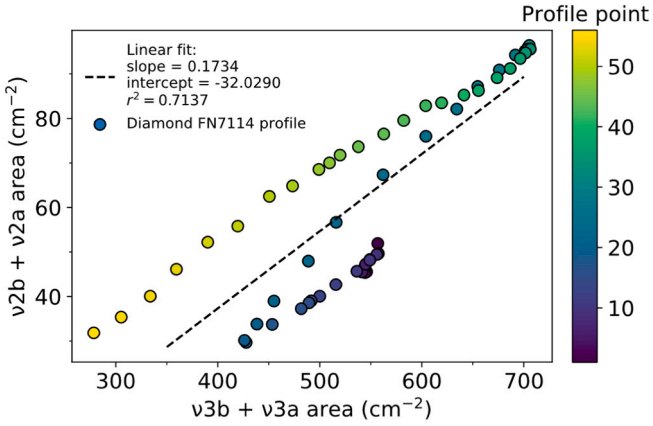

Fig. 9. Correlation of the integrated areas of $\nu_{2a} + \nu_{2b}$ and $\nu_{3b} + \nu_{3a}$ bands for diamond FN7114. Presence of several segments is explained by evolution of areas of corresponding bands along the profile. Profile points between 1–20 and 20–35 are influenced by ν_{3a} and thus deviate from linearity.

$KHCO_3$ contain numerous bands absent in our case. Nevertheless, hydrogen bonds in protonated carbonate species are among plausible species responsible for the 2415 cm^{-1} peak, since local environment of

HCO_3^- ions may lead to marked spectral variations. If this assumption is correct, behavior of this band along the profile may correspond to gradual disappearance of the protonated compounds into CO_2 and aqueous solution. A related process of diamond formation by pH drop was recently proposed by Sverjensky and Huang [37].

4.2. Shift of CO_2 IR bands

Several independent mechanisms may be responsible for blueshift of CO_2 ν_3 absorption bands and may influence their shapes: a) residual pressure; b) size, shape and eventual heterogeneous structure of CO_2 precipitates; c) strong interaction of CO_2 with matrix; d) presence of impurities in the CO_2. These possibilities are considered in detail below.

4.2.1. Pressure effects

In the case of CO_2-containing microinclusions in diamond, the most common explanation for the shifted CO_2 absorption bands is high residual pressure (e.g., [5,6,38]). Residual CO_2-I pressure may be estimated from the pressure shift of the absorption bands using the experimental data of Hofmeister and Lu [15] or Hanson and Jones [28]. In our work spectra with a CO_2 ν_{3b} area of at least 125 cm^{-2}, for which relatively precise peak position measurements were possible, were used for this purpose. The calculated pressures vary significantly for both samples. In sample FN7114 the values are 3.7–5.0 GPa (Fig. 5M). The observed positions of ν_{2a} and ν_{2b} also fit the expected values for ~4 GPa. However, the ν_{2a} pressure derivative is too small for meaningful calculations using the available data; precise determination of ν_{2b} position is difficult due to its transformation into a shoulder. For sample FN7112 only some points have ν_{3b} area of more than 125 cm^{-2}, so reported maps are incomplete. For sample FN7112 calculated pressures are 3.7–4.2 GPa (Fig. 3I).

The principal problem with the attribution of the blueshifted bands to pressure effects only lies in the peculiar spatial distribution of inferred pressures in the diamonds. This was noted already in previous works [5,6,11] and is addressed in more detail in the present work. In sample FN7112, the CO_2 bands with the largest shift (the highest inferred pressure) form irregular zones. In diamond FN7114, the inferred residual pressure increases upon approaching the nitrogen-containing zone. The nitrogen aggregation plot for the latter diamond indicates that temperature was most likely decreasing during crystallization of the N-containing zone, which is difficult to reconcile with increasing pressure. Note, however, that nitrogen may be contained in IR-inactive defects or in unidentified defects with unknown IR cross-section. The IR beam may eventually average over several growth horizons, although this contribution appears to be minor, since the trend on the Taylor plot does not show sharp or erratic changes.

From calculations based on elasticity theory, Anthony and Meng [39] suggested that certain spatial distributions of microinclusions may indeed generate stresses approaching the crushing strength of diamond and lead to plastic deformation. In principle, partial release of the residual pressure by the plastic flow might be able to explain the gradual changes of CO_2 bands positions. Chinn [5] suggested that extremely high pressures in some of diamonds are explained by partial graphitization of the inclusion walls, see Anthony [40] for relevant calculations. However, several observations indicate that pressure alone cannot be the cause of the band behavior: a) the pressure hypothesis does not explain the observed decrease of the absorption and band broadening; b) lack of correlation between the inclusions observed microscopically and the CO_2 absorption peaks casts doubt on the "stress" hypothesis. X-ray topographs of these stones shows numerous small specks, which are almost certainly due to localized strain fields surrounding hexagonal inclusions. In the same time, X-ray topography, being a sensitive method, shows rather moderate degree of deformation and distribution of stress in the samples does not follow evolution of the CO_2-related IR bands.

4.2.2. Crystallography and structure of CO_2 precipitates

In thin crystals with cubic symmetry a LO phonon may appear in transmission mode IR measurements [31]; for thin layers of CO_2 ices this was well demonstrated by Escribano et al. [41]. This effect may strongly distort the "standard" spectrum and novel peaks may appear as blueshifted bands of CO_2. It was also shown [42,43] that in core-shell CO_2-N_2O and CO_2-H_2O nanoparticles the spectral envelope very strongly depends on the thickness of the layers (particle structure), shape and composition of the particles. Some of the CO_2-diamonds from Chinn [5] (e.g., GC 859C, 727H, 790B, 874C on both presented spectra) show spectra remarkably similar to those modelled and measured by Isenor et al. [42]. Variations of composition and structure of the CO_2-containing inclusions may explain at least part of the observed complexity. We also note that, due to limited spectral resolution (2 cm^{-1}) of our experiment, variations in chemistry, shape, and stress state experienced by the CO_2-species, fine structure of the CO_2 absorption bands may be unresolved.

4.2.3. Matrix interaction

Hainschwang et al. [11] used the anomalous shifts, FWHM and intensities of bands assigned to CO_2 to propose that in the studied diamonds those features cannot be explained by microinclusions of CO_2. Instead, they suggest that exsolution of oxygen impurities in the diamonds may form CO_2 molecules and that their interaction with the diamond lattice is responsible for the observed spectral peculiarities. This scenario is qualitatively similar to the behavior of CO_2-molecules in channels present in the structure of cordierite and some other minerals (see Chukanov and Chervonnyi [20] and references therein). For the diamond case, models resembling sub-nm voids with fullerene-like walls were considered, but correspondence between the calculations and experimental spectra is, at best, qualitative [44]. Refinement of this model requires very detailed analysis of atomic structure of the void walls, not performed yet. Assignment of the observed *regular* evolution of IR bands across diamond crystals to the voids filled with pure CO_2 necessitates a mechanism of similar changes in the void structure or changes in their size distribution.

4.2.4. Influence of impurities in CO_2

A hypothesis, which, in our view, better fits experimental data, is discussed below. The presence of impurities in CO_2 ice may influence positions, width and splitting of IR features. For example, in mixed CO_2-H_2O ice an increase of water fraction from 22 to 75% leads to blueshift of the ν_3 maximum by ~10 cm^{-1} [32]. Judging solely by the position of the ν_3 maximum, such blueshift can be interpreted as an increase in pressure by ~1.5 GPa, which is obviously not the case. As already mentioned, admixture of water also leads to band broadening and a loss of ν_2 Davydov splitting occurs [32]. Raman study of fluid N_2-CO_2 inclusions in natural diamonds also suggests a strong influence of chemical composition on spectral features [7]. Examination of a profile across the FN7114 sample shows gradual evolution of position, FWHM and intensity of the CO_2-bands. In the nitrogen-rich zone CO_2-I bands become weaker, broader and shifted. All those phenomena can be explained by an increase of the impurity fraction in the CO_2 ice.

4.3. Implications for oxygen in diamond

Conclusive evidence for oxygen impurities in the diamond lattice remains elusive. However, there is a growing body of evidence that several spectroscopic features of diamonds could be related to this impurity: an optical absorption band with a peak at 480 nm [11], a peak at 1060 cm^{-1} in IR [13,45] and the 566 nm luminescence band [13]. Earlier works [6,11] indicated that the CO_2 IR absorption is stronger in regions with lower concentrations of N-related defects, see also Fig. 7A from the present study. SIMS investigation of a large set of diamonds showed the existence of a positive correlation between total N and O contents [12]. Since the former element is clearly present as a

substitutional impurity, this correlation appears to support the hypothesis of oxygen-related defects in the diamond lattice. We stress that the proportionality coefficient between N and O in SIMS data for the CO_2 and pseudo-CO_2 diamonds differs considerably from those in samples lacking CO_2 IR features. It was suggested that the coexistence of these two impurities in a given volume and their interaction prevents formation and/or hinders IR manifestations of well-known N defects and at least part of the SIMS and X-ray scattering results can be explained by formation of N-O-containing inclusions.

One of the main results of the present study is that the position and intensity of the CO_2 peaks in diamonds are not entirely random, but, instead, gradual changes and/or domains enriched in CO_2 are present. In many cases, crystallographic zoning revealed by cathodoluminescence is present [5,11]. All studies of CO_2-diamonds mention anticorrelation of the carbon dioxide features and IR-active N and H impurities in the diamond lattice. Our detailed FTIR mapping and profiling show that although some amount of structural hydrogen and nitrogen is definitely present in all parts of the studied samples as manifested by the 3107 cm^{-1} peak, the CO_2-absorption bands indeed become weaker with increased concentration of common A and B defects. Interestingly, diamond synthesis in CO_2-rich alkaline systems always is reported to produce N-rich crystals [13,46]. Incorporation of nitrogen in diamond is clearly a complex function of N speciation and abundance in the growth medium, which, in turn, depend on its composition and fO_2. Therefore, the CO_2-N(H) dependencies suggest the importance of the composition of the growth medium on the prominence of the CO_2-features. Changes of fluid chemical composition will be pronounced not only in IR spectra of hydrous fluids or melts captured by diamonds [47,48], but also in spectra of CO_2-bearing diamonds.

5. Conclusions

A detailed FTIR investigation of polished plates cut from two CO_2-rich single crystal diamonds reveals that changes of the CO_2-related IR features are not as random as it might seem from examination of bulk samples. Regular evolution of the position of the bands, FWHM and intensity is recorded for one of the samples; for the second stone, several domains with highly variable spectra are observed. Consideration of various possible mechanisms responsible for blueshift of CO_2-absorption bands suggests that the observed spectral shifts cannot be explained exclusively by the residual pressure assumption. In our view, accounting for impurities (primarily aqueous and N-containing species) in entrapped CO_2 ice is necessary for consistent explanation of the data. In future works spatially resolved spectroscopic measurements are preferred over the bulk ones, otherwise strong peak overlap may occur.

An important implication of our results is that shifts of CO_2-related bands in diamonds should be employed as a barometer with great care. If unaccounted for, impurities in CO_2 ice can introduce significant bias. In high purity CO_2-I the ν_2 band is subject to Davydov splitting. Consequently, CO_2 spectroscopic barometry gives unambiguous results only in cases when Davydov splitting of CO_2 ν_2 band is clearly observed. Schrauder and Navon [6] reported a strong asymmetry of the ν_2 CO_2 band, but in their spectrum there is no obvious Davydov splitting. This may indicate the presence of impurities in CO_2 ice in their sample. Thus, the reported residual pressure appears to be overestimated as it was calculated solely based on the position of the CO_2 bands.

Our results allow explaining the nature of CO_2 related bands in CO_2-diamonds by the presence of impure CO_2-I in microinclusions. However, this does not exclude the possibility of the presence of oxygen as a lattice impurity in diamonds.

CRediT authorship contribution statement

E.P.B. – investigation, software, data analysis, writing draft and revised version; T.H. - resources, writing draft; A.A.S. – conceptualization, methodology, investigation, writing draft and revised version. All authors have contributed to preparation and agreed to the submitted version of the manuscript.

Declaration of competing interest

The authors declare that they have no known competing financial interests or personal relationships that could have appeared to influence the work reported in this paper.

Acknowledgments

The study was partly supported by RFBR grant 13-05-91320-SIG-a to AAS. We thank Dr. A. Shapagin for access to FTIR microscope and Uladzislava Dabranskaya from Utrecht University for creation of the graphical abstract. We highly appreciate thorough consideration of the manuscript and highly useful comments made by two anonymous reviewers.

Appendix A. Supplementary data

All raw and processed FTIR spectra are available as Supplementary Materials at: “FTIR maps and profiles for CO2-rich diamonds”, Mendeley Data, V2, 10.17632/yjrgv5fhhm.2.

References

[1] C.E. Melton, C.A. Salotti, A.A. Giardini, The observation of nitrogen, water, carbon dioxide, methane, and argon as impurities in natural diamonds, Am. Mineral. 57 (1972) 1518–1523.
[2] C.E. Melton, A.A. Giardini, The composition and significance of gas released from natural diamonds from Africa and Brazil, Am. Mineral. 59 (1974) 775–782.
[3] C.E. Melton, A.A. Giardini, Experimental results and a theoretical interpretation of gaseous inclusions found in Arkansas natural diamonds, Am. Mineral. 60 (1975) 413–417.
[4] C.E. Melton, A.A. Giardini, The nature and significance of occluded fluids in three Indian diamonds, Am. Mineral. 66 (1981) 746–750.
[5] I. Chinn, A Study of Unusual Diamonds From the George Creek K1 Kimberlite Dyke, Colorado (PhD Thesis), University of Cape Town, 1995.
[6] M. Schrauder, O. Navon, Solid carbon dioxide in a natural diamond, Nature 365 (6441) (1993) 42–44, https://doi.org/10.1038/365042a0.
[7] E.M. Smith, M.G. Kopylova, M.L. Frezzotti, V.P. Afanasiev, Fluid inclusions in Ebelyakh diamonds: evidence of CO_2 liberation in eclogite and the effect of H_2O on diamond habit, Lithos 216-217 (2014) 106–117.
[8] A.A. Tomilenko, A.I. Chepurov, Y.N. Pal’yanov, L.N. Pokhilenko, A.P. Shebanin, Volatile components in the upper mantle (from data on fluid inclusions), Russ. Geol. Geophys. 38 (1997) 294–303.
[9] D.K. Voznyak, V.N. Kvasnitsa, T. Ya Kislyakova, Liquefied gases in natural diamond, Geochemistry International 29 (9) (1992) 107–112 (Translated from Geokhimiya, 29(2), 268–273).
[10] T. Hainschwang, N. Franck, F. Emmanuel, M. Laurent, M.B. Christopher, B. Rondeau, Natural “CO_2-rich” colored diamonds, Gems & Gemology, Fall 2006 (2006) 97.
[11] T. Hainschwang, F. Notari, E. Fritsch, L. Massi, B. Rondeau, C.M. Breeding, H. Vollstaedt, HPHT treatment of CO_2 containing and CO_2-related brown diamonds, Diam. Relat. Mater. 17 (3) (2008) 340–351, https://doi.org/10.1016/j.diamond.2008.01.022.
[12] A.A. Shiryaev, M. Wiedenbeck, T. Hainschwang, Oxygen in bulk monocrystalline diamonds and its correlations with nitrogen, J. Phys.: Condens. Matter 22 (2010) 045801–045806.
[13] Y.N. Palyanov, I.N. Kupriyanov, A.G. Sokol, Y.M. Borzdov, A.F. Khokhryakov, Effect of CO_2 on crystallization and properties of diamond from ultra-alkaline carbonate melt, Lithos 265 (2016) 339–350, https://doi.org/10.1016/j.lithos.2016.05.021.
[14] M. Wojdyr, Fityk: a general-purpose peak fitting program, J. Appl. Crystallogr. 43 (5) (2010) 1126–1128, https://doi.org/10.1107/S0021889810030499.
[15] R. Lu, A.M. Hofmeister, Infrared fundamentals and phase transitions in CO_2 up to 50 GPa, Phys. Rev. B 52 (6) (1995) 3985–3992, https://doi.org/10.1103/PhysRevB.52.3985.
[16] W.E. Osberg, D.F. Hornig, The vibrational spectra of molecules and complex ions in crystals. VI. Carbon dioxide, J. Phys. Chem. 20 (1952) 1345–1347, https://doi.org/10.1063/1.1700760.
[17] J.P. Goss, P.R. Briddon, V. Hill, R. Jones, M.J. Rayson, Identification of the structure of the 3107 cm^{-1} H-related defect in diamond, J. Phys.: Condens. Matter 26 (14) (2014), 145801, https://doi.org/10.1088/0953-8984/26/14/145801.
[18] S.R. Boyd, I. Kiflawi, G.S. Woods, Infrared absorption by the B nitrogen aggregate in diamond, Philos. Mag. B 72 (3) (1995) 351–361.

[19] I. Kiflawi, A.E. Mayer, P.M. Spear, J.A. van Wyk, G.S. Woods, Infrared absorption by the single nitrogen and a defect centres in diamond, Phil. Mag. B 69 (6) (1994) 1141–1147.
[20] N.V. Chukanov, A.D. Chervonnyi, Infrared Spectroscopy of Minerals and Related Compounds, Springer, 2016.
[21] J.D. Hunter, Matplotlib: a 2D graphics environment, Comput. Sci. Eng. 9 (3) (2007) 90–95.
[22] A.R. Lang, G.P. Bulanova, D. Fisher, S. Furkert, A. Sarua, Defects in a mixed-habit Yakutian diamond: studies by optical and cathodoluminescence microscopy, infrared absorption, Raman scattering and photoluminescence spectroscopy, J. Crystal Growth 309 (2007) 170–180.
[23] T. Hainschwang, F. Notari, G. Pamies, A defect study and classification of brown diamonds with non-deformation-related color, Minerals 10 (2020) 914, https://doi.org/10.3390/min10100914.
[24] J.L. Birman, Theory of crystal space groups and infra-red and Raman lattice processes of insulating crystals, in: Theory of Crystal Space Groups and Lattice Dynamics, Springer, Berlin, Heidelberg, 1974, https://doi.org/10.1007/978-3-642-69707-4_1.
[25] M.Y. Lai, T. Stachel, C.M. Breeding, R.A. Stern, Yellow diamonds with colourless cores – evidence for episodic diamond growth beneath Chidliak and the Ekati Mine, Canada, Mineralogy and Petrology 114 (2020) 91–103.
[26] W.R. Taylor, A.L. Jaques, M. Ridd, Nitrogen-defect aggregation characteristics of some Australasian diamonds: time-temperature constraints on the source regions of pipe and alluvial diamonds, Amer. Miner. 75 (1990) 1290–1310.
[27] H. Olijnyk, A.P. Jephcoat, Vibrational studies on CO_2 up to 40 GPa by Raman spectroscopy at room temperature, Phys. Rev. B 57 (2) (1998) 879–888, https://doi.org/10.1103/PhysRevB.57.879.
[28] R.C. Hanson, L.H. Jones, Infrared and Raman studies of pressure effects on the vibrational modes of solid CO_2, J. Phys. Chem. 75 (1981) 1102–1112, https://doi.org/10.1063/1.442183.
[29] G.A. Baratta, M.E. Palumbo, The profile of the bending mode band in solid CO_2, Astronomy & Astrophysics 608 (2017) A81 (9 pp).
[30] D.A. Dows, V. Schettino, Two-phonon infrared absorption spectra in crystalline carbon dioxide, J. Phys. Chem. 58 (1973) 5009–5016, https://doi.org/10.1063/1.1679088.
[31] D.W. Berreman, Infrared absorption at longitudinal optic frequency in cubic crystal films, Phys. Rev. 130 (6) (1963) 2193–2198.
[32] I.R. Cooke, E.C. Fayolle, K.I. Öberg, CO_2 infrared phonon modes in interstellar ice mixtures, Astrophys. J. 832 (1) (2016) 5 (8 pp), https://doi.org/10.3847/0004-637X/832/1/5.
[33] W. Zheng, R.I. Kaiser, On the formation of carbonic acid (H_2CO_3) in solar system ices, Chem. Phys. Lett. 450 (2007) 55–60.
[34] G. Lucazeau, A. Novak, Low temperature Raman spectra of $KHCO_3$ single crystal, J. Raman Spectrosc. 1 (1973) 573–586, https://doi.org/10.1002/jrs.1250010607.
[35] E.H. Abramson, O. Bollengier, J.M. Brown, Water-carbon dioxide solid phase equilibria at pressures above 4 GPa, Sci. Rep. 7 (2017) 821, https://doi.org/10.1038/s41598-017-00915-0.
[36] H. Wang, J. Zeuschner, M. Eremets, I. Troyan, J. Willams, Stable solid and aqueous H_2CO_3 from CO_2 and H_2O at high pressure and high temperature, Sci. Rep. 6 (2016) 19902, https://doi.org/10.1038/srep19902.
[37] D.A. Sverjensky, F. Huang, Diamond formation due to a pH drop during fluid–rock interactions, Nature Comm. 6 (2015) 8702, https://doi.org/10.1038/ncomms9702.
[38] A.A. Shiryaev, K. Iakoubovskii, D. Grambole, N.D. Dubrovinskaia, Spectroscopic study of defects and inclusions in bulk poly- and nanocrystalline diamond aggregates, J. Phys.: Condens. Matter 18 (2006) L493–L501.
[39] T.R. Anthony, Y. Meng, Stresses generated by inhomogeneous distributions of inclusions in diamonds, Diam. Relat. Mater. 6 (1997) 120–129.
[40] T.R. Anthony, The behavior of gas inclusions in diamond generated by temperature changes, Diam. Relat. Mater. 4 (1994) 83–94.
[41] R.M. Escribano, G.M. Muñoz Caro, G.A. Cruz-Diaz, Y. Rodríguez-Lazcano, B. Maté, Crystallization of CO_2 ice and the absence of amorphous CO_2 ice in space, Proc. Nat. Acad. Sci 110 (32) (2013) 12899–12904.
[42] M. Isenor, R. Escribano, T.C. Preson, R. Signorell, Predicting the infrared band profiles for CO_2 cloud particles on Mars, Icarus 223 (1) (2013) 591–601.
[43] R. Signorell, M. Jetzki, M. Kunzmann, R. Ueberschaer, Unraveling the origin of band shapes in infrared spectra of N_2O-$^{12}CO_2$ and $^{12}CO_2$-$^{13}CO_2$ ice particles, J. Phys. Chem. A 110 (9) (2006) 2890–2897, https://doi.org/10.1021/jp053021u.
[44] J.-J. Adjizian, C.D. Latham, M.I. Heggie, P.R. Briddon, M.J. Rayson, S. Öberg, Infrared signatures of CO2 in diamond from first principles, in: Ext. Abstracts, 60th De Beers Diamond Conference, 2009.
[45] V.G. Malogolovets, N.I. Nikityuk, Vibrational frequencies of diamond lattice induced by substitutional impurities, Superhard Materials 5 (1978) 28–31.
[46] A.F. Khokhryakov, Y.N. Palyanov, I.N. Kupriyanov, D.V. Nechaev, Diamond crystallization in a CO_2-rich alkaline carbonate melt with a nitrogen additive, J. Crystal Growth 449 (2016) (2016) 119–128.
[47] Y. Weiss, I. Kiflawi, O. Navon, The IR absorption Spectrum of water in microinclusion-bearing diamonds, in: D.G. Pearson (Ed.), Proceedings of 10th International Kimberlite Conference vol. 1, 2013 (Special Issue of the Journal of the Geological Society of India).
[48] D.A. Zedgenizov, A.A. Shiryaev, V.S. Shatsky, H. Kagi, Water-related IR characteristics in natural fibrous diamonds, Min. Mag. 70 (2006) 219–229.